Spin transitions in graphene butterflies at an integer filling factor

Areg Ghazaryan and Tapash Chakraborty*
Department of Physics and Astronomy, University of Manitoba, Winnipeg, Canada R3T 2N2
(Received 8 December 2014; published 19 March 2015)

Recent experiments on the role of electron-electron interactions in fractal Dirac systems have revealed a host of interesting effects, in particular, the unique nature of the magnetic field dependence of butterfly gaps in graphene. The novel gap structure recently observed in the integer quantum Hall effect is quite intriguing [G. L. Yu *et al.*, Nat. Phys. **10**, 525 (2014)], where one observes a suppression of the ferromagnetic state at one value of the commensurable flux but a reentrant ferromagnetic state at another. In our present work we introduce the magnetic translation symmetry in the integer quantum Hall effect regime and consider the interplay between the electron-electron interaction and the periodic potential. In this approach, we explain the underlying physical processes that can lead to such a unique behavior of the butterfly gaps as observed in that system where we invoke the spin-flip transitions in the ground state.

DOI: 10.1103/PhysRevB.91.125131 PACS number(s): 71.10.Pm, 73.20.At, 73.21.Cd

I. INTRODUCTION

The fascinating dynamics of Dirac fermions in graphene has been exhaustively studied in recent years [1–3]. Coulomb interaction between Dirac fermions [4], in particular, in the presence of a strong perpendicular magnetic field has resulted in the fractional quantum Hall states in monolayer [5] and bilayer graphene [6], which have also been experimentally observed [7]. Graphene placed on boron nitride with a twist displays fractal butterflies [8,9] of Dirac fermions [10] when subjected to a perpendicular magnetic field. After the exciting discovery of the fractal butterflies in graphene [11–13] in 2013, more recent theoretical [14] and experimental [15] studies have focused on the influence of electron-electron interactions on the butterfly gaps. Given the intricacies of these gaps, the interaction effects are, quite expectedly, more complex in the integer and the fractional quantum Hall effect regime, where one observes an interplay between the quantum Hall effect gap and the Hofstadter gap [16].

In studying the interaction effects in the integer quantum Hall effect regime, Yu *et al.* [15] employed capacitance spectroscopy to explore the "Hofstadter minigaps" for zero and integer filling factors. Their results for the energy gaps at filling factors $\nu = 0, \pm 1$ ($\nu = n\phi_0/B$, n is the particle density, and ϕ_0 is the flux quantum) showed very unusual magnetic field dependence. In the low-magnetic-field region, the $\nu = 0$ gap rises *linearly* with B and saturates near the magnetic flux value $\phi = \phi_0/2$ but exhibits a minimum at $\phi = \phi_0$. Additionally, they have also explored the energy gaps for the first Landau level (LL), and their results show that for filling factor $\nu = 4$ the gap shows oscillating behavior (see the Supplementary Information in [15]). It again rises linearly with B for low magnetic fields, reaches the maximum value at around the magnetic flux value $\phi = \phi_0/3$, and then goes to almost zero at $\phi = \phi_0/2$. After that the same behavior is repeated in the region of $\phi = \phi_0/2$ to $\phi = \phi_0$. Therefore for both the zeroth and the first LLs the gap deviates significantly from the Coulomb energy in several regions, thereby indicating that the transitions across the gap from the ground state do not necessarily involve the particle charge alone.

By employing the magnetic translation group algebra [17] in the quantum Hall effect regime [16,18–20], we have analyzed the magnetic field dependence of the $\nu = 0$ and $\nu = 4$ butterfly gaps. Our results reveal that the observed gap structure involves spin-flip transitions in the ground state, as explained below, and can be used to analyze the magnetic field dependence of the energy gaps for filling factors $\nu = 0$ and $\nu = 4$, as observed in Ref. [15].

II. THEORETICAL FRAMEWORK

In what follows, we consider monolayer graphene in an external periodic potential [14,21–23]

$$V(x,y) = V_0[\cos(q_x x) + \cos(q_y y)], \tag{1}$$

where V_0 is the amplitude of the periodic potential and $q_x = q_y = q_0 = 2\pi/a_0$, where a_0 is the period of the external potential. Then the many-body Hamiltonian is

$$\mathcal{H} = \sum_i^{N_e} \left[\mathcal{H}_B^i + V(x_i, y_i)\right] + \frac{1}{2}\sum_{i\neq j}^{N_e} V_{ij}, \tag{2}$$

where $\mathcal{H}_B^i$ is the Hamiltonian of an electron in graphene in a perpendicular magnetic field and the last term is the Coulomb interaction. The electron energy spectrum of graphene has twofold valley and twofold spin degeneracy in the absence of an external magnetic field, the periodic potential and the interaction between the electrons. It is well known [1,2] that for magnetic fields that are presently accessible in the experiments, the conservation of the SU(2) valley symmetry in the presence of the Coulomb interaction is a fully justified approximation. We therefore employ this approximation in our studies. In order for the external periodic potential to break the SU(2) valley symmetry, the scattering process will require momentum transfer comparable to the value of the difference of momentum between the two valleys. The period of the external potential accessible in the experiment for the moiré superlattice is much bigger than the graphene lattice constant. Therefore the probability for such a momentum transfer process is exponentially small and can be disregarded.

*tapash.chakraborty@umanitoba.ca

In order to investigate the optimum state of total valley and real spin that is favored by the system in our calculations, we consider both the spin and valley degrees of freedom of the electron system. Here the spin degeneracy is lifted due to the Zeeman effect, while in the approximation described above there is no term in the Hamiltonian (2) that lifts the valley degeneracy. The single-particle Hamiltonian $\mathcal{H}_B$ is then written as [1–3]

$$\mathcal{H}_B = \xi v_F \begin{pmatrix} 0 & \pi_- \\ \pi_+ & 0 \end{pmatrix} + \frac{1}{2} g_e \mu_B B \sigma_z, \tag{3}$$

where $\pi_\pm = \pi_x \pm i\pi_y$, $\boldsymbol{\pi} = \mathbf{p} + e\mathbf{A}/c$, $\mathbf{p}$ is the two-dimensional electron momentum, $\mathbf{A} = (0, Bx, 0)$ is the vector potential, $v_F \approx 10^6$ m/s is the Fermi velocity in graphene, and the last term is the electron Zeeman energy. The ξ is the valley index: $\xi = 1$ for valley K and $\xi = -1$ for valley K'. The honeycomb lattice of graphene consists of two sublattices A and B, and the two-component wave functions corresponding to the Hamiltonian (3) can be expressed as $(\psi_A, \psi_B)^T$ for valley K and $(\psi_B, \psi_A)^T$ for valley K', where ψ_A and ψ_B are wave functions of sublattices A and B, respectively. The eigenfunction of the Hamiltonian (3) for both K and K' valleys can be written in the form [1–3]

$$\Psi_{n,j} = C_n \begin{pmatrix} \mathrm{sgn}(n)(-i)\varphi_{|n|-1,j} \\ \varphi_{|n|,j} \end{pmatrix}, \tag{4}$$

where $C_n = 1$ for $n = 0$ and $C_n = 1/\sqrt{2}$ for $n \neq 0$, $\mathrm{sgn}(n) = 1$ for $n > 0$, $\mathrm{sgn}(n) = 0$ for $n = 0$, and $\mathrm{sgn}(n) = -1$ for $n < 0$. Here $\varphi_{n,j}$ is the electron wave function in the nth LL with the parabolic dispersion, taking into account the periodic boundary conditions (PBC) [20,24]

$$\varphi_{n,j}(x,y) = \frac{1}{\sqrt{L_y \pi^{1/2} \ell_0 2^n n!}} \sum_{k=-\infty}^{\infty} e^{\frac{i}{\ell_0^2}(X_j + kL_x)y} \times e^{-\frac{(x+kL_x+X_j)^2}{2\ell_0^2}} H_n\left(\frac{x + kL_x + X_j}{\ell_0}\right), \tag{5}$$

where $X_j = 2\pi j \ell_0^2 / L_y$, $\ell_0 = \sqrt{c\hbar/eB}$ is the magnetic length, $H_n(x)$ are the Hermite polynomials, and L_x and L_y describe the size of the system. The eigenvalues of the Hamiltonian (3) without the Zeeman term and corresponding to the eigenvectors (4) for both valleys K and K' are $\epsilon_n = \mathrm{sgn}(n)\hbar\omega_B\sqrt{|n|}$, where $\omega_B = \sqrt{2}v_F/\ell_0$.

III. MAGNETIC TRANSLATION ANALYSIS

We now develop the magnetic translation algebra [16,18–20] which will be used to characterize the states of the many-body Hamiltonian (2) and will let us bring the many-body Hamiltonian matrix into block diagonal form using the eigenvectors of the appropriate magnetic translations. The single-particle translation operator which commutes with the Hamiltonian (3) has the form

$$\tau(\mathbf{a}) = \begin{pmatrix} e^{-\frac{i}{\hbar}\mathbf{a}\cdot\mathbf{K}} & 0 \\ 0 & e^{-\frac{i}{\hbar}\mathbf{a}\cdot\mathbf{K}} \end{pmatrix}, \tag{6}$$

where $\mathbf{K} = -\mathbf{p} - eBy\hat{\mathbf{x}}/c$. Since the magnetic translation operator (6) is diagonal in its components, we will develop the algebra for only one component of the diagonal matrix. Using the Baker-Campbell-Hausdorff formula, it can be shown that

$$T(\mathbf{a}) = e^{-\frac{i}{\hbar}\mathbf{a}\cdot\mathbf{K}} = e^{\frac{i}{\ell_0^2}(a_x y + \frac{1}{2}a_x a_y)} e^{\frac{i}{\hbar}\mathbf{a}\cdot\mathbf{p}}. \tag{7}$$

The application of the PBC implies that the wave function $\varphi_{n,j}$ is the eigenvector of the translation operator $T(\mathbf{L}_{mn})$, where $\mathbf{L}_{mn} = mL_x\hat{\mathbf{x}} + nL_y\hat{\mathbf{y}}$ defines the magnetic translation lattice vector and m,n are integers. In addition, it results in j of X_j in (5) taking integer values in the range $0 \leqslant j < N_s$, where $L_xL_y = 2\pi N_s \ell_0^2$ and N_s is the number of flux quanta piercing through the magnetic translation lattice cell or, alternatively, describes the LL degeneracy for each value of the spin and valley indices and takes integer values. The maximal set of translations which both commutes with the Hamiltonian (3) and acts within a given Hilbert space described by the eigenvectors (5) is the set $\{\mathbf{L}_{mn}/N_s\}$ [18,20].

In the presence of an additional periodic potential the size of the system is expressed as $L_x = M_x a_0$ and $L_y = M_y a_0$ (M_x and M_y are integers). Defining the parameter $\alpha = \phi_0/\phi$, where $\phi = Ba_0^2$ is the magnetic flux through the unit cell of the periodic potential and $\phi_0 = hc/e$ is the flux quantum, we have

$$\frac{N_s}{M_x M_y} = \frac{1}{\alpha} = \frac{r}{v}, \tag{8}$$

where r and v are coprime integers. Before the application of PBC, the single-particle Hamiltonian which includes the periodic potential is symmetric under the translations with the periodic potential lattice vector $T(\mathbf{a}_{uw})$, where $\mathbf{a}_{uw} = ua_0\hat{\mathbf{x}} + wa_0\hat{\mathbf{y}}$ and u and w are again integers. In order to have this symmetry after the application of PBC the translations with the periodic potential lattice vector $T(\mathbf{a}_{uw})$ and the magnetic translation lattice vector $T(\mathbf{L}_{mn})$ must commute. This condition results in additional constraints on our system that M_x and M_y are divisible by v. These constraints and (8) dictate that $N_s = \kappa_{x,y} M_{x,y}$, where $\kappa_{x,y}$ are integers. Therefore for the case with the periodic potential the maximal set of translations which both commutes with the single-particle Hamiltonian (periodic potential included) and acts within the same Hilbert space described by the eigenvectors (5) is the subset of $\{\mathbf{L}_{mn}/N_s\}$ with the elements which are also translations by the periodic potential lattice vector.

We now analyze the magnetic translation algebra for a many-body system in the presence of the external periodic potential. We consider a system of a finite number N_e of electrons again in a toroidal geometry similar to the case of a single electron, i.e., the size of the system is again $L_x = M_x a_0$ and $L_y = M_y a_0$ (M_x and M_y are integers), and we apply PBC in order to eliminate the boundary effects. Although this analysis is quite general and can be used for any filling factor of the system, in this work we consider the filling factors $\nu = 0$ and $\nu = 4$. This means that the number of electrons in the appropriate LL if both valleys are included is $N_e = 2N_s$ due to the fourfold degeneracy of each LL in graphene, and $N_e = N_s$ if only the K valley is considered.

Based on the above considerations we search for the appropriate translations to characterize the states of the many-body Hamiltonian (2) in the form of the center-of-mass (c.m.)

translations, which are defined as

$$T^{\text{c.m.}}(\mathbf{a}) = \prod_{i=1}^{N_e} T_i(\mathbf{a}), \tag{9}$$

with the translation vector $\mathbf{a}_p = m\beta_1 a_0 \hat{\mathbf{x}} + n\beta_2 a_0 \hat{\mathbf{y}}$, where β_1 and β_2 are integers to be determined below. It can easily be shown that the c.m. translation $T^{\text{c.m.}}(\mathbf{a_p})$ commutes both with the many-body Hamiltonian (2) and with the translation $T_i(\mathbf{L}_{mn})$ for any particle i. Additionally, it also acts within the same Hilbert space described by the many-body states $|j_1, j_2, \ldots, j_{N_e}\rangle$ (besides j_i, each single-particle state is characterized by the LL, spin, and valley indices, which are not shown but are implicitly assumed to be included in the indices j_i) which are constructed from the single-particle eigenvectors (4). In order for these c.m. translations to be diagonalized simultaneously, i.e., the c.m. translations commute with each other, the following condition must be satisfied:

$$\frac{N_e \beta_1 \beta_2}{\alpha} = \pm 1, \pm 2, \ldots, \tag{10}$$

where $\beta_1\beta_2$ describes the degeneracy of the system for each value of the c.m. momentum. By choosing, for example, $\beta_2 = 1$ and demanding the above condition for β_1, it can be shown that this condition is the same as the one obtained earlier by Kol and Read [19].

We now make the assumption that the application of the normal momentum operator $\mathcal{Q}(\mathbf{Q}) = \sum_i e^{i\mathbf{Q}\cdot\mathbf{r}_i}$ to the many-particle state will increase its momentum by $\mathbf{Q}$ provided that $\mathbf{Q}$ is allowed by PBC, i.e., it is a magnetic translation reciprocal-lattice vector. From the relation

$$T^{\text{c.m.}}(\mathbf{a}_p)\mathcal{Q}(\mathbf{Q}_{st}) = e^{i\mathbf{a}_p\cdot\mathbf{Q}_{st}}\mathcal{Q}(\mathbf{Q}_{st})T^{\text{c.m.}}(\mathbf{a}_p), \tag{11}$$

it follows that the eigenvalues of the c.m. translation operator will have the form $e^{2\pi i(\beta_1 ms/M_x + \beta_2 nt/M_y)}$, where s and t are integers which characterize the vector $\mathbf{Q}_{st}$ in a magnetic translation reciprocal lattice. Hence s and t are defined only modulo M_x/β_1 and M_y/β_2, respectively, and there are $M_xM_y/\beta_1\beta_2$ allowed eigenvalues. It is clear from the discussions above that s and t are related to the c.m. momentum of the system. We then factorize the c.m. translation operator $T^{\text{c.m.}}(\mathbf{a_p})$ into two parts,

$$T^{\text{c.m.}}(\mathbf{a}_p) = (-1)^{N_e\beta_1\beta_2 mn/\alpha} T^{\text{c.m.}}(\beta_1 m a_0 \hat{\mathbf{x}}) T^{\text{c.m.}}(\beta_2 n a_0 \hat{\mathbf{y}}), \tag{12}$$

and calculate how the constituents in the factorization act on the many-body state $|j_1, j_2, \ldots, j_{N_e}\rangle$,

$$T^{\text{c.m.}}(\beta_2 n a_0 \hat{\mathbf{y}})\left|j_1, j_2, \ldots, j_{N_e}\right\rangle = e^{i2\pi\frac{\beta_2 n}{M_y}t}\left|j_1, j_2, \ldots, j_{N_e}\right\rangle, \tag{13}$$

$$T^{\text{c.m.}}(\beta_1 m a_0 \hat{\mathbf{x}})\left|j_1, j_2, \ldots, j_{N_e}\right\rangle = \left|j_1 + m\beta_1\kappa_x, j_2 + m\beta_1\kappa_x, \ldots, j_{N_e} + m\beta_1\kappa_x\right\rangle, \tag{14}$$

where $t = \sum_i j_i \bmod (M_y/\beta_2)$ is the total momentum quantum number in the y direction. We then use these results to construct the eigenstates of the c.m. translation $T^{\text{c.m.}}(\mathbf{a_p})$ based on the procedure outlined previously in Ref. [20] for the case without the periodic potential. This means we fix the total momentum t and construct the set $\mathcal{T}$ of all the N_e particle states with the momentum t, i.e., $\mathcal{T} = \{|j_1, j_2, \ldots, j_{N_e}\rangle| \quad 0 \leqslant j_i < N_s, \quad \sum_i j_i = t \bmod (M_y/\beta_2)\}$. We then divide the set $\mathcal{T}$ into equivalence classes by defining the states $|j_1', j_2', \ldots, j_{N_e}'\rangle$ and $|j_1, j_2, \ldots, j_{N_e}\rangle$ equivalent iff they are related by the rule

$$\left|j_1', j_2', \ldots, j_{N_e}'\right\rangle = \left|j_1 + m\beta_1\kappa_x, j_2 + m\beta_1\kappa_x, \ldots, j_{N_e} + m\beta_1\kappa_x\right\rangle. \tag{15}$$

It can easily be seen that these equivalence classes can contain at most M_x/β_1 members because the momenta j_i are defined (mod N_s). Let $\mathcal{L}$ be one such set represented by the state $|j_1, j_2, \ldots, j_{N_e}\rangle$. It is clear from the construction that the members of this set are mapped back to the set by the translation operators $T^{\text{c.m.}}(\beta_1 m a_0 \hat{\mathbf{x}})$ and $T^{\text{c.m.}}(\beta_2 n a_0 \hat{\mathbf{y}})$ and therefore by any translation operator $T^{\text{c.m.}}(\mathbf{a}_p)$. Based on the above consideration we assert that the complete set of normalized states

$$|(s,t)\rangle = \frac{1}{\sqrt{|\mathcal{L}|}} \sum_{k=0}^{|\mathcal{L}|-1} e^{-i2\pi\frac{\beta_1 s}{M_x}k} \times \left|j_1 + \beta_1\kappa_x k, j_2 + \beta_1\kappa_x k, \ldots, j_{N_e} + \beta_1\kappa_x k\right\rangle \tag{16}$$

forms the set of the eigenstates of $T^{\text{c.m.}}(\mathbf{a}_p)$. Using these eigenstates of the c.m. translations, we can divide the Hamiltonian matrix constructed from the Hamiltonian operator (2) and the many-body states $|j_1, j_2, \ldots, j_{N_e}\rangle$ into block diagonal form where each block is diagonalized separately. It also allows us to identify each eigenvalue of the Hamiltonian with the c.m. translation $T^{\text{c.m.}}(\mathbf{a}_p)$ eigenvalue and therefore with the appropriate c.m. momentum. Hence, using the c.m. translation analysis, the Hamiltonian matrix can be approximately divided into $M_xM_y/\beta_1\beta_2$ separate blocks, which can then be diagonalized using the exact diagonalization procedure.

IV. RESULTS AND DISCUSSION

In what follows we consider the two cases $\alpha = 1$ and $\alpha = 2$ that were studied in the experiment [15]. We then choose the system size based on condition (8) and the number of electrons. After comparing the results for small system sizes in the cases with and without the inclusion of the contribution of higher LLs, in what follows we disregard the LL mixing and present all the results for the $n = 0$ LL for $\nu = 0$ and the $n = 1$ LL for $\nu = 4$. Here we present the results for three system sizes, $N_e = 8$, taking into account both K and K' valleys; $N_e = 6$, taking into account only the K valley for $\nu = 0$; and $N_e = 8$, again taking into account only the K valley for both $\nu = 0$ and $\nu = 4$. For $N_e = 8$ in two valleys the system size is $M_x = 2$ and $M_y = 2$ for $\alpha = 1$ and $M_x = 4$ and $M_y = 2$ for $\alpha = 2$. For $N_e = 6$ in one valley the system size is $M_x = 3$ and $M_y = 2$ for $\alpha = 1$ and $M_x = 6$ and $M_y = 2$ for $\alpha = 2$, and for $N_e = 8$ in one valley the system size is $M_x = 4$ and $M_y = 2$ for $\alpha = 1$ and $M_x = 4$ and $M_y = 4$ for $\alpha = 2$. In order to investigate the magnetic field dependence of the gap we fix the value of α and change the magnetic field B and the period of the periodic potential simultaneously.

In Fig. 1 the dependence of the gap between the ground state and the first excited state on the magnetic field strength is presented for $N_e = 8$ electrons and $\nu = 0$ in K and K' valleys

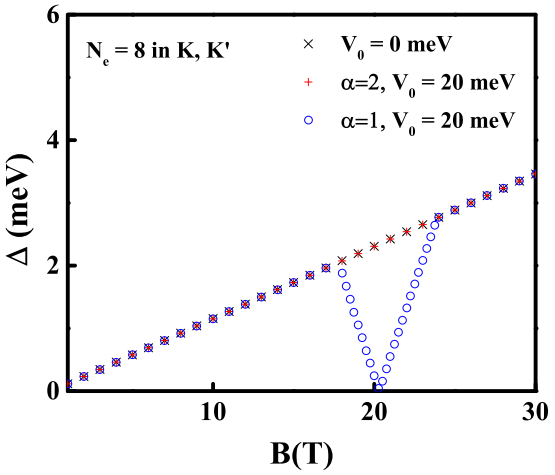

FIG. 1. (Color online) The gap between the ground and the first excited states of an eight-electron system in two valleys vs the magnetic field B for $\nu = 0$ with $V_0 = 20$ meV, $\alpha = 1,2$, and also without the external periodic potential.

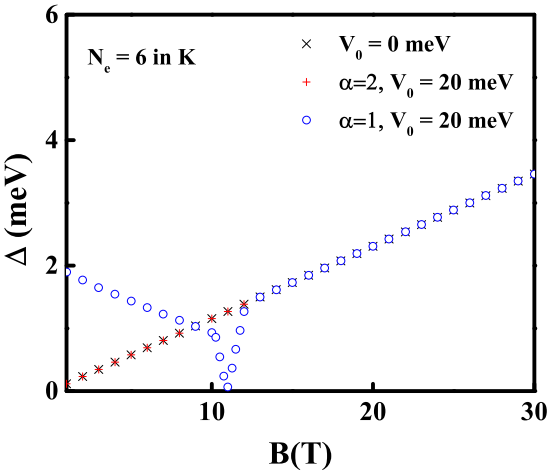

FIG. 2. (Color online) Same as in Fig. 1, but for the system of six electrons. Only the K valley is considered in this case.

for $\alpha = 1$ and for $\alpha = 2$ with $V_0 = 20$ meV and without the periodic potential. In the absence of the periodic potential the change of α results only in the change of geometry of the system and therefore does not have any contribution in the gap value, and in the figures the $V_0 = 0$ case is presented without the indication of the value of α. For $V_0 = 0$ and for all values of the magnetic field the ground state corresponds to four electrons in each valley, with all electrons having their spins in the direction opposite to the magnetic field. In the excited state we have seven spin-down electrons and one spin-up electron. This excited state is degenerate because the spin-up electron can be in either of the two valleys, i.e., either in the one where the three spin-down electrons are or in the one where there are four spin-down electrons. It should also be noted that there is no momentum transfer in this transition from the ground state to the excited state described above, which means that both the ground and excited states have the same total momentum (equal to zero) and the gap is equal to the Zeeman energy of the spin flip. Therefore for $V_0 = 0$ the electron-electron interaction does not have any contribution in the lowest gap of the system. As can be seen from Fig. 1, surprisingly, the situation remains the same for $\alpha = 2$ and $V_0 = 20$ meV.

For $\alpha = 1$ and $V_0 = 20$ meV the situation is remarkably different. In the magnetic field region up to 18 T the ground state has $S_z = -2$ and there are four electrons in each valley. This corresponds to the case when in each valley three electrons have spin down and one electron spin up. Therefore, the periodic potential changes the ground state of the system from the fully spin polarized state to the spin partially polarized state in this case. In the excited state $S_z = -1$, which again means one additional spin flip, and again the level is degenerate with respect to the exchange of spin-up parts between the valleys. In Fig. 1 the gap is again equal to the Zeeman energy of the spin flip. At $B \approx 18$ T there is a crossing between the first and the second excited states and up to $B = 20$ T the first excited state has $S_z = -4$, and the gap corresponds to the transition between the states with double spin flip from the spin up to down and is again equal to the Zeeman energy of that transition. At $B \approx 20$ T there is a crossing between the ground and the first excited states, and after that the ground state is the state with $S_z = -4$. The first excited state is the state with $S_z = -2$ up to 24 T and the state with $S_z = -3$ (which is again degenerate due to the different configurations of the spin-up states between two valleys) afterwards. For these two parts, the gap is again equal only to the Zeeman energy for the appropriate transition. It should be noted that in the range of magnetic fields considered in this case both the ground and the excited states are described by the total momentum equal to zero, and there is no momentum transfer in these transitions. Although the gap energy in this case is always equal to the Zeeman energy of the appropriate transition, the gap structure shown for $\alpha = 1$ and $V_0 = 20$ meV is not the single-particle effect. Both the electron-electron interaction and the periodic potential are essential for the system to deviate from the ferromagnetic state at low magnetic fields and afterwards for the observation of the transition from a spin partially polarized state to the fully polarized spin state by increasing the magnetic field.

In Figs. 2 and 3 the dependence of the gap between the ground state and the first excited state on the magnetic

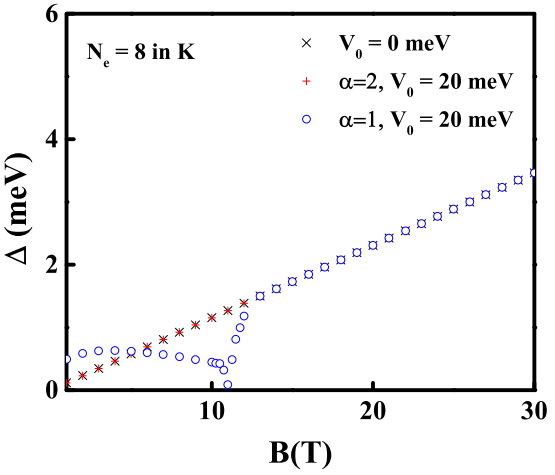

FIG. 3. (Color online) Same as in Fig. 2, but for the system of eight electrons. Only the K valley is considered in this case.

field strength is presented for $N_e = 6$ and $N_e = 8$ electrons, $\alpha = 1$ and $\alpha = 2$, with $V_0 = 20$ meV and without the periodic potential and for filling factor $\nu = 0$. Only the K valley is considered in these cases. The cases of $V_0 = 0$ and $V_0 = 20$ meV with $\alpha = 2$ show the same behavior as for $N_e = 8$ electrons in the K and K' valleys shown in Fig. 1. The ground state is ferromagnetic for all values of the magnetic field, and the gap corresponds to the transition to the excited state with a single spin flip. For $\alpha = 1$ and $V_0 = 20$ meV the situation is different. For small magnetic fields (up to 10 T) the ground state has $S_z = 0$ (spin unpolarized state), and the transition corresponds to the excited state with $S_z = -1$. It should be noted that in addition to the spin flip, there is also the momentum transfer in these transitions because the first excited stated is characterized by a nonzero momentum up to 10 T. Therefore these transitions correspond to the *collective excitations*, and the gap energy comprises both the Zeeman term and the $\Delta \propto \sqrt{B}$ term. This structure is clearly visible for the $N_e = 8$ electron case, but for the $N_e = 6$ electron case the collective nature of the excitation is completely suppressed by the Zeeman term for magnetic fields considered in Fig. 2. In Figs. 2 and 3, starting with $B = 10$ T, the structure of the transition is the same as that for the case of $N_e = 8$ electrons in the K and K' valleys shown in Fig. 1. There are several crossings between the low-lying states, and the ground state of the system changes from the spin-unpolarized ground state to the ferromagnetic (fully polarized) state. In the ferromagnetic regime the gap again corresponds to the spin flip and is equal to the Zeeman energy of that flip.

In Fig. 4 the dependence of the gap between the ground state and the first excited state on the magnetic field strength is presented for $N_e = 8$ electrons, $\alpha = 1$ and $\alpha = 2$, with $V_0 = 20$ meV and without the periodic potential and for the filling factor $\nu = 4$. Only the K valley is considered in these cases. While the dependence of the gap for $V_0 = 0$ is the same as that for the $\nu = 0$ filling factor, in the case of $\nu = 4$ and $V_0 = 20$ meV and $\alpha = 1,2$ there is a transition from the partially spin polarized or the unpolarized ground state to the fully polarized (ferromagnetic) ground state with the increase of the magnetic field. When $\alpha = 2$, the system is initially in the partially spin polarized ground state with $S_z = -2$, and the transition corresponds to the excited state with $S_z = -1$. Starting from $B \approx 10$ T, again, several crossings take place in the low-lying states, and at $B \approx 12$ T the system becomes the ferromagnetic ground state. This transition is similar to the case of $\alpha = 1$ of Fig. 1 because for all values of the magnetic field considered, both the ground and excited states are described with the same total momentum, so the gap energy is comprised only from Zeeman term for the appropriate transition. For $\alpha = 1$ the system is initially in the spin-unpolarized ground state with $S_z = 0$, and the transition is to the excited state with $S_z = -1$. By increasing the magnetic field to $B \approx 19$ T the system again becomes the ferromagnetic state. This case is similar to that of $\alpha = 1$ in Fig. 2 or Fig. 3 because up to the $B \approx 18$ T the transition involves total momentum change (collective excitation), and the gap energy again comprises both the Zeeman term and the $\Delta \propto \sqrt{B}$ term. After the passage to the ferromagnetic state the gap energy is described again solely by the Zeeman term.

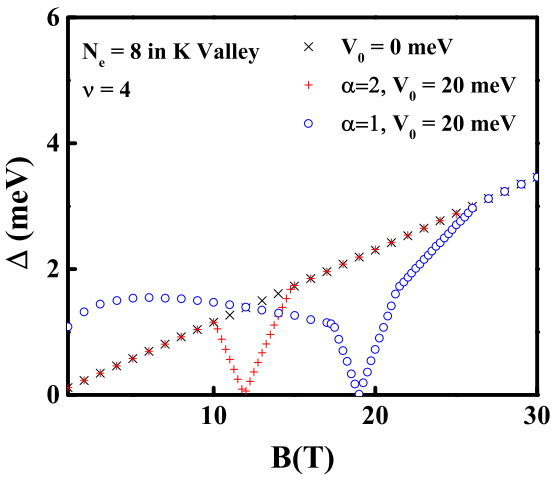

FIG. 4. (Color online) Same as in Fig. 2, but for the filling factor $\nu = 4$. Only the K valley is considered in this case.

We now use the features observed in this work to interpret the result shown in Figs. 4 and S4 of Ref. [15] (for Fig. S4 see the Supplementary Information in Ref. [15]) for the filling factors $\nu = 0$ and $\nu = 4$. For filling factor $\nu = 0$ and magnetic fields up to 20 T, due to the valley anisotropic terms [25] and also due to the spin-unpolarized state observed for low magnetic fields in our work, the system is presumably in a spin-unpolarized state. The almost linear dependence of the gap at magnetic fields up to around 5 T and the $\sqrt{B}$ dependence for magnetic fields between 5 and 20 T indicate that the excitations have both spin-flip and momentum transfer components (collective excitation). Based on these observations, it can be assumed that there is a competition between these two components and that for up to 5-T magnetic fields the Zeeman contribution is dominant in the gap energy, whereas in the range of magnetic fields from 5 to 20 T the electron-electron interaction contribution is dominant. The lowering of the gap in the region close to $\alpha = 1$, then almost linear dependence after around 28 T, coupled with the absence of similar features for $\alpha = 2$ closely resembles the results obtained in our paper. We therefore suggest that this behavior indicates that there is a phase transition around $\alpha = 1$; that is, there is a transition from the spin-unpolarized state to the partially or fully spin polarized state. Similar reasoning can be applied for the $\nu = 4$ case, where for the magnetic fields up to 8 T ($\phi = \phi_0/3$) the energy gap increases linearly and then decreases to zero at 12 T ($\phi = \phi_0/2$). Similar behavior is observed also in the range of 12–24 T ($\phi = \phi_0/2$ to $\phi = \phi_0$), although the dependence slightly deviates from the linear dependence. Observation of similar features for both $\alpha = 1$ and $\alpha = 2$ in our results for $\nu = 4$ strongly supports our analysis and indicates that the system is again in a spin-unpolarized or partially polarized state for low magnetic fields and makes the transition to another partially polarized state at $\phi = \phi_0/2$ and a partially or fully polarized state at $\phi = \phi_0$.

V. CONCLUSION

In conclusion, we have considered the influence of the periodic potential due to the moiré lattice on the dependence of the energy gap on the magnetic field for filling factors $\nu = 0$

and $\nu = 4$ in graphene using the exact diagonalization scheme. We have considered three cases: $N_e = 8$ electrons in the K and K' valleys and $N_e = 6$ and $N_e = 8$ electrons located only in the K valley and disregarding the contribution of the K' valley. In all cases for $\nu = 0$ we find that for $\alpha = 1$, inclusion of the periodic potential and the electron-electron interactions results in an unpolarized or partially polarized ground state in lower magnetic fields and a transition to the fully polarized ground state by increasing the magnetic field. This behavior is not observed for the $\alpha = 2$ case, where we observe only the ferromagnetic state for all values of the magnetic field. In contrast to the case of $\nu = 0$, for $\nu = 4$ the transition from the unpolarized or the partially polarized ground state to the fully polarized ground state by increasing the magnetic field is observed for both the $\alpha = 1$ and $\alpha = 2$ cases. The similarity between the results obtained here and those reported in Figs. 4 and S4 in Ref. [15] was analyzed, and a possible explanation was presented on the behavior of the dependence of the gap on the perpendicular magnetic field observed in that work.

ACKNOWLEDGMENTS

This work has been supported by the Canada Research Chairs Program of the Government of Canada.

[1] *Physics of Graphene*, edited by H. Aoki and M. S. Dresselhaus (Springer, New York, 2014).
[2] D. S. L. Abergel, V. Apalkov, J. Berashevich, K. Ziegler, and T. Chakraborty, Adv. Phys. **59**, 261 (2010).
[3] T. Chakraborty and V. Apalkov, in *Physics of Graphene* (Ref. [1]), Chap. 8; Solid State Commun. **175-176**, 123 (2013).
[4] V. Apalkov and T. Chakraborty, Solid State Commun. **177**, 128 (2014); D. S. L. Abergel and T. Chakraborty, Phys. Rev. Lett. **102**, 056807 (2009); D. S. L. Abergel, V. M. Apalkov, and T. Chakraborty, Phys. Rev. B **78**, 193405 (2008); D. S. L. Abergel, P. Pietiläinen, and T. Chakraborty, *ibid.* **80**, 081408(R) (2009); V. M. Apalkov and T. Chakraborty, *ibid.* **86**, 035401 (2012).
[5] V. M. Apalkov and T. Chakraborty, Phys. Rev. Lett. **97**, 126801 (2006).
[6] V. M. Apalkov and T. Chakraborty, Phys. Rev. Lett. **105**, 036801 (2010); **107**, 186803 (2011).
[7] X. Du, I. Skachko, F. Duerr, A. Luican, and E. Y. Andrei, Nature (London) **462**, 192 (2009); D. A. Abanin, I. Skachko, X. Du, E. Y. Andrei, and L. S. Levitov, Phys. Rev. B **81**, 115410 (2010); K. I. Bolotin, F. Ghahari, M. D. Shulman, H. L. Störmer, and P. Kim, Nature (London) **462**, 196 (2009); F. Ghahari, Y. Zhao, P. Cadden-Zimansky, K. Bolotin, and P. Kim, Phys. Rev. Lett. **106**, 046801 (2011).
[8] D. Langbein, Phys. Rev. **180**, 633 (1969).
[9] D. Hofstadter, Phys. Rev. B **14**, 2239 (1976).
[10] T. Chakraborty and V. M. Apalkov, IET Circuits Devices Syst. **9**, 19 (2015).
[11] C. R. Dean, L. Wang, P. Maher, C. Forsythe, F. Ghahari, Y. Gao, J. Katoch, M. Ishigami, P. Moon, M. Koshino, T. Taniguchi, K. Watanabe, K. L. Shepard, J. Hone, and P. Kim, Nature (London) **497**, 598 (2013).
[12] B. Hunt, J. D. Sanchez-Yamagishi, A. F. Young, M. Yankowitz, B. J. LeRoy, K. Watanabe, T. Taniguchi, P. Moon, M. Koshino, P. Jarillo-Herrero, and R. C. Ashoori, Science **340**, 1427 (2013).
[13] L. A. Ponomarenko, R. V. Gorbachev, G. L. Yu, D. C. Elias, R. Jalil, A. A. Patel, A. Mishchenko, A. S. Mayorov, C. R. Woods, J. R. Wallbank, M. Mucha-Kruczynski, B. A. Piot, M. Potemski, I. V. Grigorieva, K. S. Novoselov, F. Guinea, V. I. Falko, and A. K. Geim, Nature (London) **497**, 594 (2013).
[14] V. M. Apalkov and T. Chakraborty, Phys. Rev. Lett. **112**, 176401 (2014).
[15] G. L. Yu, R. V. Gorbachev, J. S. Tu, A. V. Kretinin, Y. Cao, R. Jalil, F. Withers, L. A. Ponomarenko, B. A. Piot, M. Potemski, D. C. Elias, X. Chen, K. Watanabe, T. Taniguchi, I. V. Grigorieva, K. S. Novoselov, V. I. Falko, A. K. Geim, and A. Mishchenko, Nat. Phys. **10**, 525 (2014).
[16] A. Ghazaryan, T. Chakraborty, and P. Pietiläinen, arXiv:1408.3424.
[17] J. Zak, Phys. Rev. **134**, A1602 (1964); E. Brown, *ibid.* **133**, A1038 (1964)
[18] F. D. M. Haldane, Phys. Rev. Lett. **55**, 2095 (1985).
[19] A. Kol and N. Read, Phys. Rev. B **48**, 8890 (1993).
[20] T. Chakraborty and P. Pietiläinen, *The Quantum Hall Effects* (Springer, New York, 1995); *The Fractional Quantum Hall Effect* (Springer, New York, 1988).
[21] U. Rössler and M. Shurke, Adv. Solid State Phys. **40**, 35 (2000).
[22] V. Gudmundsson and R. R. Gerhardts, Surf. Sci. **361-362**, 505 (1996); Phys. Rev. B **52**, 16744 (1995); **54**, R5223 (1996).
[23] M. Koshino and T. Ando, J. Phys. Soc. Jpn. **73**, 3243 (2004).
[24] The periodic rectangular geometry was extensively used earlier in the study of the fractional quantum Hall effect in various situations. For example, see T. Chakraborty, Surf. Sci. **229**, 16 (1990); Adv. Phys. **49**, 959 (2000); T. Chakraborty and P. Pietiläinen, Phys. Rev. Lett. **76**, 4018 (1996); **83**, 5559 (1999); Phys. Rev. B **39**, 7971 (1989); V. M. Apalkov, T. Chakraborty, P. Pietiläinen, and K. Niemelä, Phys. Rev. Lett. **86**, 1311 (2001); T. Chakraborty, P. Pietiläinen, and F. C. Zhang, *ibid.* **57**, 130 (1986); T. Chakraborty and F. C. Zhang, Phys. Rev. B **29**, 7032(R) (1984); F. C. Zhang and T. Chakraborty, *ibid.* **30**, 7320(R) (1984).
[25] D. A. Abanin, B. E. Feldman, A. Yacoby, and B. I. Halperin, Phys. Rev. B **88**, 115407 (2013).